The Plant Cell, Vol. 6, 1253–1264, September 1994 © 1994 American Society of Plant Physiologists

Control of Leaf and Chloroplast Development by the Arabidopsis Gene *pale cress*

Robert S. Reiter, Shirley A. Coomber,[1] Timothy M. Bourett, Glenn E. Bartley, and Pablo A. Scolnik[2]

Du Pont Central Research, P.O. Box 80402, Wilmington, Delaware 19880-0402

Leaf plastids of the Arabidopsis *pale cress* (*pac*) mutant do not develop beyond the initial stages of differentiation from proplastids or etioplasts and contain only low levels of chlorophylls and carotenoids. Early in development, the epidermis and mesophyll of *pac* leaves resemble those of wild-type plants. In later stages, mutant leaves have enlarged intercellular spaces, and the palisade layer of the mesophyll can no longer be distinguished. To study the molecular basis of this phenotype, we cloned *PAC* and determined that this gene is regulated by light and has the capacity to encode an acidic, predominantly α-helical protein. The *PAC* gene appears to be a novel component of a light-induced regulatory network that controls the development of leaves and chloroplasts.

INTRODUCTION

Leaves develop from shoot meristem cells that contain proplastids, colorless organelles with little internal structure that are precursors of chloroplasts. As meristem cells divide and develop into cells of the leaf, proplastids differentiate into chloroplasts. The development of organs and organelles in plants is a separate (Reiss et al., 1983; Mayfield and Taylor, 1987; Taylor, 1989; Zhang et al., 1992) but coordinated (Hou et al., 1993) process. This is supported by the observation that genetic or chemical blocks in chloroplast development have no direct effect on leaf morphology. In agreement with this observation, we determined that among chloroplast mutants identified in a collection of Agrobacterium-treated Arabidopsis mutants (Feldmann, 1991), leaf morphology is generally unaffected. However, a small percentage of these mutants show alterations in leaf development, suggesting the existence of nuclear genes required for both chloroplast and leaf differentiation. The characterization of these mutants may lead to a new understanding of the coordination between leaf and chloroplast development. Here, we report the cellular and molecular characterization of *pale cress* (*pac*), a mutant of this group.

RESULTS

Isolation and Characterization of *pac*

To identify mutants blocked in chloroplast development, we screened a collection of 8000 Arabidopsis T-DNA insertional mutants (Feldmann, 1991). We identified 300 lines with pale green, yellow, or albino cotyledons that germinate normally, indicating that embryo morphogenesis is not affected. Before mutant seedlings die as a result of the lack of photosynthesis, primary leaves can be seen differentiating from the apical meristem. When plated on nutrient agar, most mutant seedlings developed morphologically normal but unpigmented or pale leaves. However, 6 to 10 of these mutants also showed alterations in leaf development that resulted in the formation of leaf blades that were clearly thinner than the wild type. From this class we selected *pac*, a pale green mutant shown in Figure 1, for further characterization.

To characterize the photosynthetic pigments of *pac* mutants, we extracted total chlorophylls and carotenoids. As indicated in Table 1, mutant plants accumulate chlorophylls *a* and *b* and carotenoids at less than 3% of wild-type levels. Using thin-layer chromatography, we detected chlorophylls *a* and *b* and the colored carotenoids lutein, β-carotene, neoxanthin, and violaxanthin. Leaves of mature *pac* plants showed a decrease in opacity and substance that, as explained below, is a result of alterations in leaf development. In developing siliques of selfed heterozygous *pac* plants, ~25% of the seeds did not accumulate significant amounts of chlorophyll, indicating that the *PAC* gene is also required for chloroplast formation during embryogenesis, although embryo development per se is not affected by the *PAC* deficiency. The pattern of anthocyanin deposition in seedlings was normal (data not shown), and when provided with a carbon source, these seedlings developed rosettes of normal phyllotaxy. The time of flowering of *pac* plants in sucrose media was similar to that of the wild type, and mutant plants showed no signs of premature senescence.

Plastid Development

Chloroplasts develop from proplastids through a process that involves an increase in volume and membrane expansion. In

[1] Current address: Division of Life Sciences, King's College, London W8 7AH, U.K.

[2] To whom correspondence should be addressed at Du Pont Experimental Station, Route 141 and Rising Sun Avenue, Building 402 Room 4245, Wilmington, DE 19880-0402.

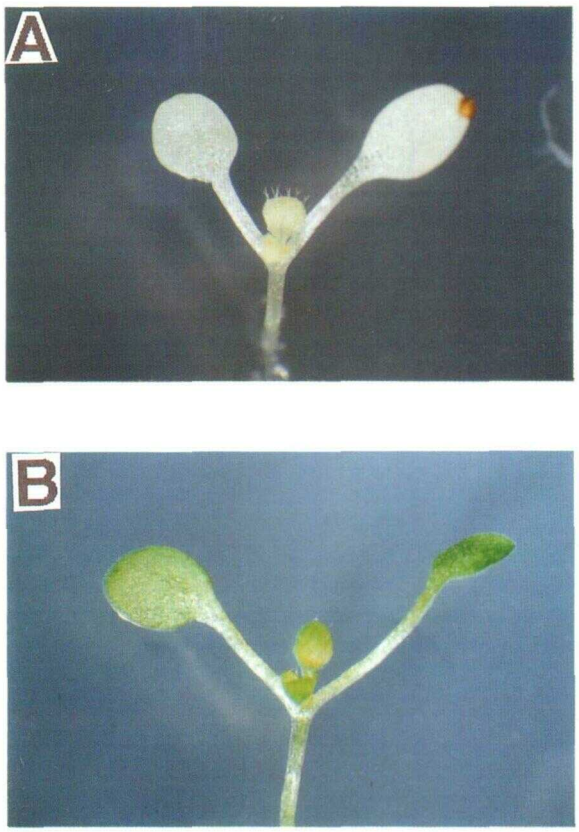

Figure 1. Wild-Type and *pac* Plants.

Seeds from a heterozygous (+/*pac*) plant were sown on nutrient agar Petri dishes and photographed 10 days after germination.
(A) Seedling of a homozygous *pac* mutant.
(B) Seedling of a green (genotype +/−) plant.
Magnification for **(A)** and **(B)** = ×10.

the mature chloroplast, internal membranes are present as either single stroma thylakoids or appressed grana thylakoids (Kirk, 1978; Staehelin, 1986). We used electron microscopy to examine plastids in cells of the apical meristem, leaf primordia, and developing leaves at stages 1 (1.5 to 2.5 mm in length) and 2 (4.0 to 5.0 mm in length). Figures 2A and 2B show that *pac* meristematic cells contain proplastids similar to those of the wild type. In leaf primordia, wild-type chloroplasts show a rudimentary thylakoid organization into grana (Figure 2C), whereas *pac* plastids show only a few lamellae that, in the example shown in Figure 2D, form a stack. This reduced stacking was not seen in every plastid (complete serial sections were not examined), but it represents the highest level of stacking observed in *pac* mesophyll plastids. In stage 1 leaves, wild-type chloroplasts are fully developed (Figure 2E), but *pac* plastids show only a reduced membrane system (Figure 2F). It is important to note that, although mutant plastids expand during leaf development, they do not reach wild-type size in mature leaves.

Plants grown in the dark form etioplasts, plastids of irregular shape with characteristic prolamellar bodies. When illuminated, the prolamellar bodies lose their crystalline structure, thylakoids become more abundant, and grana start to form. We examined mutant and wild-type plastids during a 24-hr de-etiolation experiment. Figure 3 shows electron micrographs of representative plastids at 0, 4, and 24 hr after illumination of etiolated seedlings. Prolamellar bodies and characteristic single thylakoids were clearly visible in mutant plastids (Figure 3B), which were morphologically similar to wild-type plastids at time 0 (Figure 3A). After 4 hr of illumination, both advanced dispersal of prolamellar bodies and an increase in single thylakoids were evident in both wild-type and mutant plastids (Figures 3C and 3D). At 24 hr, however, there were significant differences in plastid morphology between wild-type and *pac* leaves (Figures 3E and 3F). Mutant plastids show less thylakoid development than does the wild type at 4 hr and retain the irregular shape of etioplasts. In contrast, wild-type plastids at this stage have advanced thylakoid stacking, and grana formation is evident. Thus, *PAC* controls chloroplast differentiation from both proplastids and etioplasts.

Leaf Development

To determine the cellular basis for the leaf phenotype of *pac*, we used light microscopy to examine the structures of wild-type and mutant leaves. The sections shown in Figures 4A and 4B indicate that both wild-type and *pac* leaves have distinct epidermis, palisade, and spongy mesophyll layers at stage 1. At stage 2, epidermal and mesophyll cells and intercellular spaces of wild-type leaves have enlarged considerably (Figure 4C). However, in *pac* leaves the palisade layer is no longer apparent, many of the epidermal cells are irregularly shaped, intercellular spaces are large, and the thickness of the leaf is uneven (Figure 4D).

The analysis of the size and distribution of cells in transversely sectioned leaves shown in Table 2 indicates significant alterations in the development of *pac* leaves. At stage 1, the epidermal layers of wild-type and *pac* mutants are of similar size, but at stage 2 the volume occupied by the epidermis of *pac* mutants is more than 30% greater than that of the wild type. The average *pac* epidermal cell size is similar to the wild

Table 1. Pigment Content of *pac* Mutants

Sample	Chl *a*[a]	Chl *b*[a]	Carotenoids[a]
Wild Type	6.10 ± 0.60	1.60 ± 0.20	1.30 ± 0.10
pac	0.05 ± 0.01	0.03 ± 0.01	0.04 ± 0.01

[a] Total pigments were extracted from stage 1 plants and analyzed as given in Methods and are expressed as milligrams per gram dry weight of tissue ± SD.

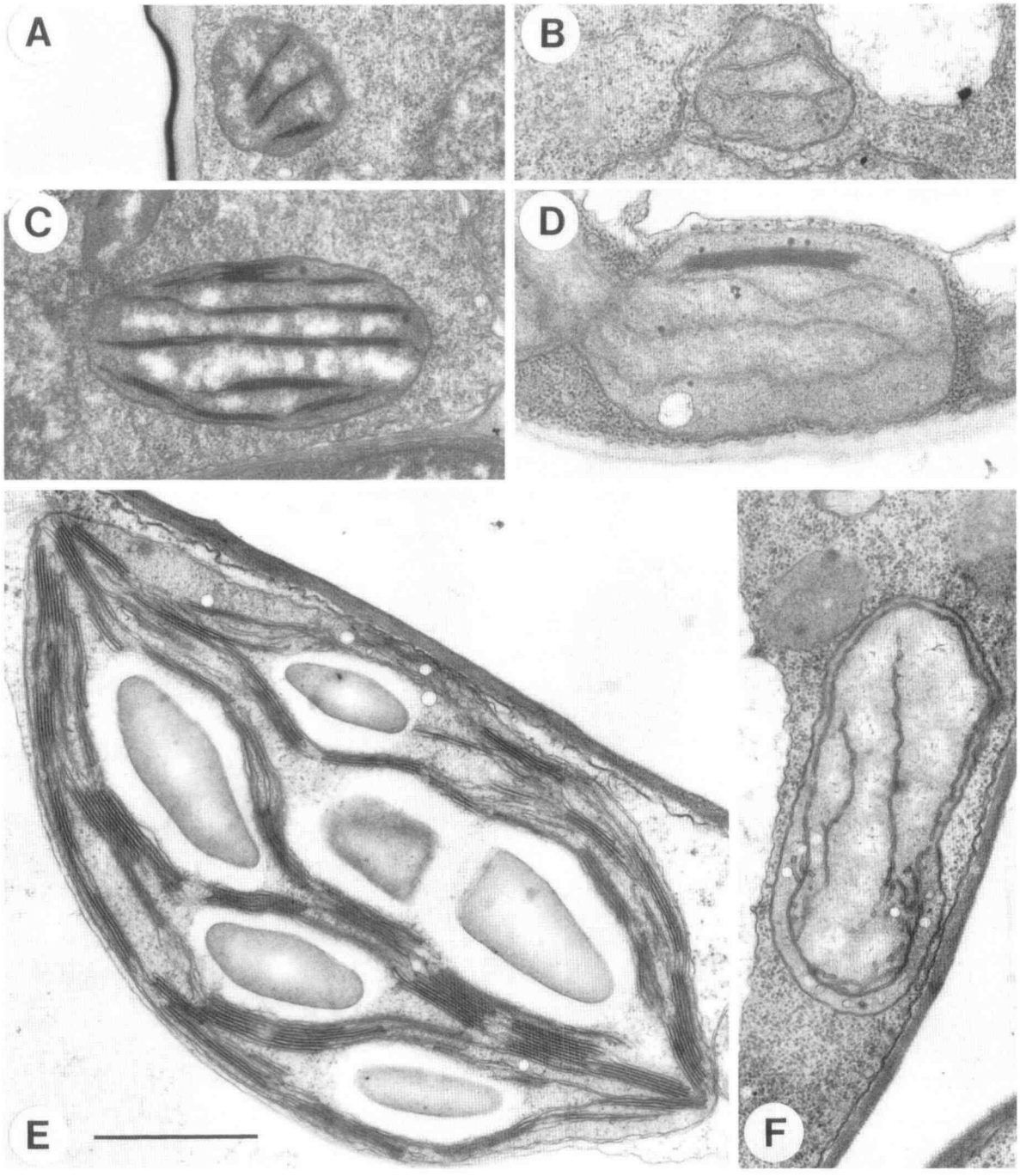

Figure 2. Ultrastructure of Leaf Plastid Development from Meristem Proplastids.

(A) Proplastid of a wild-type apical meristem cell.
(B) Proplastid of a *pac* apical meristem cell.
(C) Plastid of a wild-type leaf primordium.
(D) Plastid of a *pac* leaf primordium.
(E) Chloroplast of a stage 1 wild-type leaf.
(F) Plastid of a *pac* stage 1 leaf.
Bar in **(E)** = 1.0 μm and applies to all panels.

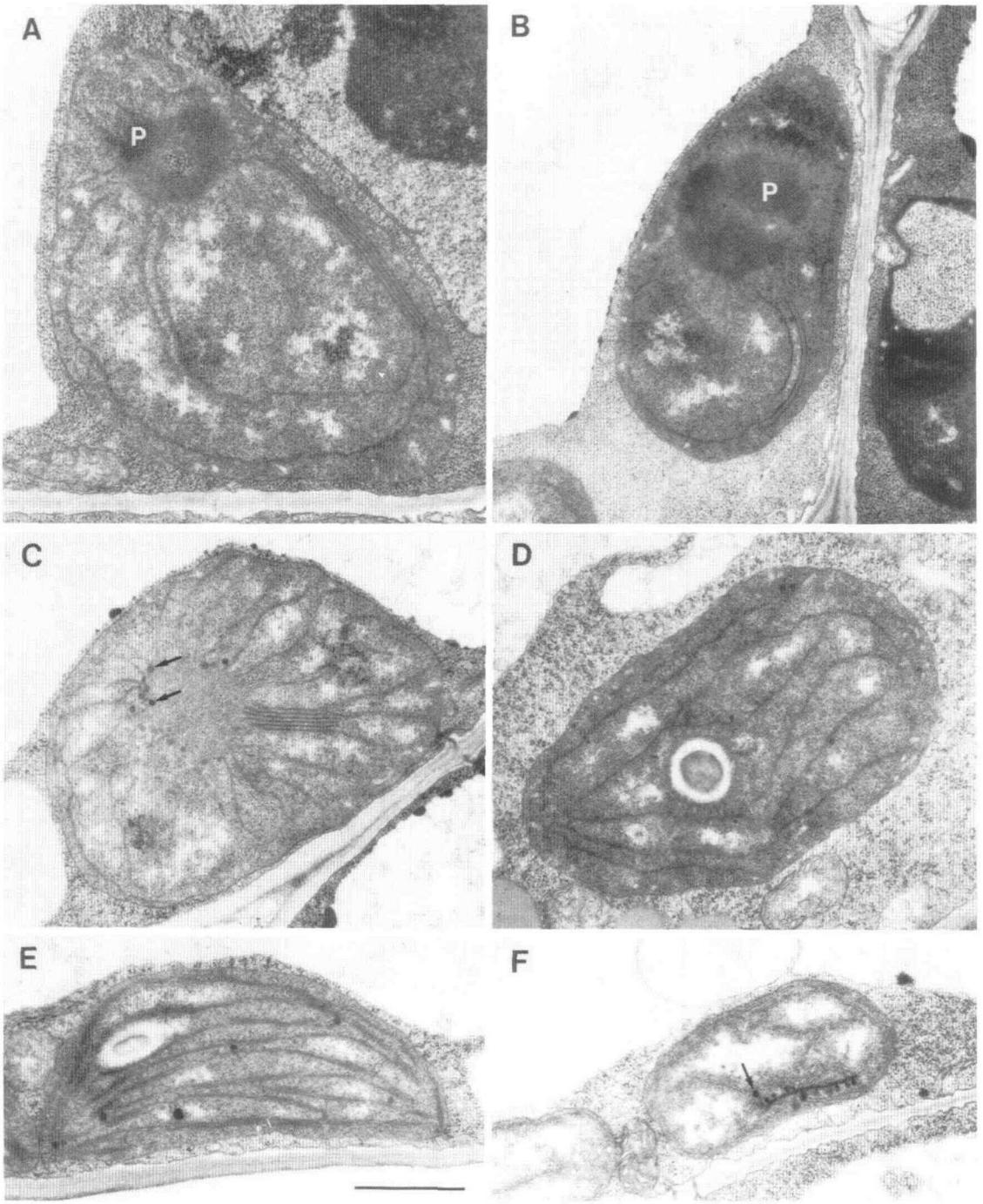

Figure 3. Ultrastructure of Plastids during De-etiolation.

(A) Etioplast of a wild-type plant grown in the dark.
(B) Etioplast of a *pac* mutant.
(C) Plastid of a wild-type plant de-etiolated for 4 hr.
(D) Plastid of a *pac* plant de-etiolated for 4 hr.
(E) Chloroplast of a wild-type plant after 24 hr of de-etiolation.
(F) Plastid of a *pac* mutant after 24 hr of de-etiolation.
Arrows indicate osmiophilic globules. P, prolamellar body.
Bar in **(E)** = 1.0 μm and applies to all panels.

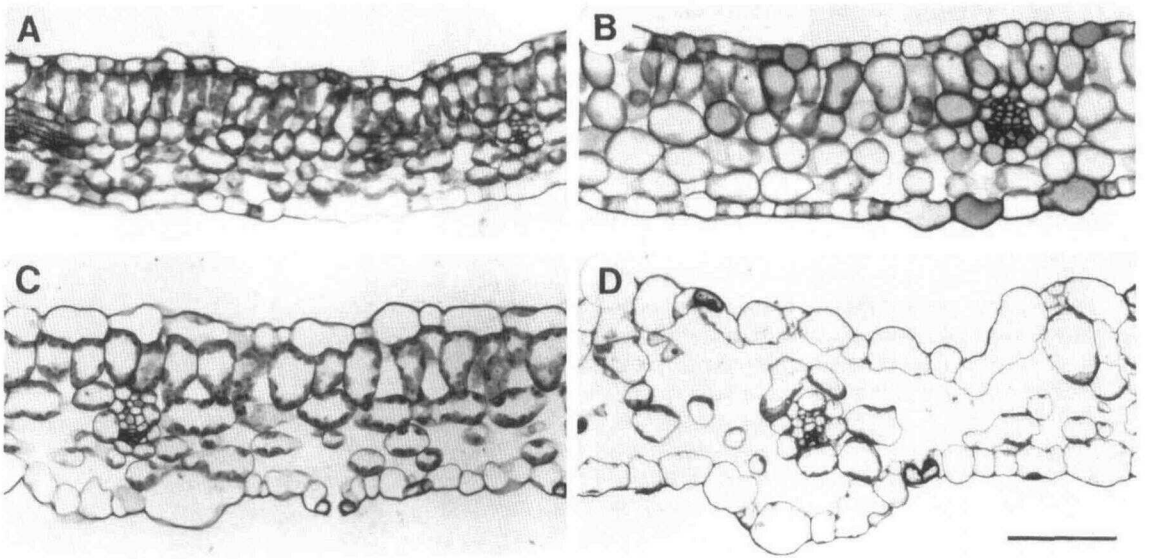

Figure 4. Light Microscopy of Leaf Development in *pac* and Wild-Type Plants.

(A) Stage 1 wild-type leaf.
(B) Stage 1 *pac* leaf.
(C) Stage 2 wild-type leaf.
(D) Stage 2 *pac* leaf.
Note the absence of a palisade layer in **(D)**. This alteration did not affect the integrity of the samples for TEM.
Bar in **(D)** = 50 μm and applies to all panels.

type at stage 1, but it is almost 40% greater than that of the wild type at stage 2. Thus, mutant epidermal cells expand more than their wild-type counterparts, resulting in a proportionally larger epidermal layer. An examination of mesophyll development revealed that at stage 1 the *pac* mesophyll layer occupies a volume equivalent to 56% of the total, whereas the corresponding wild-type volume is 63%. By stage 2, the mesophyll volume of mutant leaves is only 22.6% of the total versus 51.3% for the wild type. The analysis of cell densities indicated that at stage 1 the *pac* value is 75% of the corresponding wild-type value, and at stage 2 there are almost 50% fewer cells per unit volume in mutant versus wild-type leaves. Thus, the *pac* mutation affects the number but not the size of mesophyll cells. We did not observe any evidence of cell lysis in the

Table 2. Leaf Development in *pac* and Wild-Type Plants

			Stage 1[a]		Stage 2[a]	
Space	Tissue	Cell	Wild Type	*pac*	Wild Type	*pac*
Cellular	Epidermis	Area[b]	25.30 ± 0.95	24.50 ± 0.93	30.20 ± 0.65	39.80* ± 2.17
		Size[c]	119.14 ± 11.47	133.10 ± 9.41	206.70 ± 13.19	284.08* ± 21.14
		Density[d]	9.06 ± 0.80	7.84 ± 0.52	5.03 ± 0.33	3.68* ± 0.25
	Mesophyll	Area[b]	63.70 ± 1.03	56.20* ± 2.88	51.30 ± 1.16	22.60* ± 1.52
		Size[c]	213.52 ± 8.80	247.71* ± 13.19	315.71 ± 10.21	311.92 ± 26.05
		Density[d]	4.06 ± 0.18	3.08* ± 0.20	2.36 ± 0.10	1.25* ± 0.09
Intercellular		Area[b]	11.00 ± 1.50	19.30* ± 4.30	18.50 ± 3.00	37.60* ± 3.50

[a] Values shown are the mean and standard error for each set of observations. Mean values within each stage were compared using the student's *t*-test. Significant differences ($\alpha = 0.05$) between wild type and *pac* are indicated by asterisks. A total of 14 leaves from each wild-type and *pac* plant were sampled.
[b] As a percentage of the total area.
[c] As average cell area in square microns.
[d] As average number of cells per 1000 μm^2.

sections examined; therefore, it is likely that the lower density of mesophyll cells reflects a premature cessation of cell division. The volume occupied by the intercellular space in the mesophyll layer of mutant leaves was higher than in the wild type for both stages (75 and 203% for stages 1 and 2, respectively) and is thus largely consistent with the measurements of the cellular layers.

In summary, during the stages analyzed the program of cell division and expansion was active in *pac* mutants for both mesophyll and epidermal cells. However, cells of the *pac* epidermis expanded further than the wild-type epidermal cells, whereas mutant and wild-type mesophyll cells were similar in size, but *pac* leaves had fewer mesophyll cells per unit volume than did the wild type, and the characteristic shape of the palisade was lost by stage 2. Stage 1 *pac* leaves had a palisade (Figure 4B) but chloroplast development was arrested (see Figure 2F). Thus, in the temporal development of mutant leaves the block in chloroplast differentiation precedes the loss of the palisade layer.

Genetic Mapping and Cloning of the *PAC* Gene

We used phenotypic marker lines to map *pac* to a chromosomal location. Segregation of the pale green phenotype in 106 individual F_2 plants showed no significant deviation from the expected 3:1 ratio. Analysis of the linkage data indicates that *pac* maps to chromosome 2 at ~2 centimorgans from *cer8* and ~21.6 centimorgans from *er*. To determine linkage to the T-DNA, we plated 13,243 plants derived from heterozygous parents in agar medium containing kanamycin and scored for pigment phenotype (green or pale green) and kanamycin resistance. The segregation ratios were highly consistent with a 1:2:1 ratio, and we did not find pale green and kanamycin-sensitive plants, a phenotype that would indicate genetic recombination between the T-DNA and the *pac* mutation.

As indicated above, genetic segregation analysis suggested that *PAC* is tagged by a T-DNA. Genomic gel blot analyses (data not shown) indicated that the mutant line contains an inverted repeat T-DNA flanked by two right border sequences. To isolate DNA corresponding to this region, we cloned an EcoRI fragment carrying a pBR322 replicon and an ampicillin resistance gene and 6 kb of genomic DNA flanking the T-DNA insertion. This fragment was used as a probe to clone a 17-kb genomic DNA fragment. An 8-kb XhoI subclone was later shown to contain the entire *PAC* coding region plus flanking sequences (3.2 kb 5′ and 1.0 kb 3′). This fragment was introduced into homozygous *pac* mutants by Agrobacterium-mediated transformation (Márton and Browse, 1991). As shown in Figure 5A, the wild-type DNA fragment complemented the pigment phenotype of *pac*. Mutant plants regenerated from tissue culture have a pale green phenotype (Figure 5B), whereas wild-type plants regenerated under the same conditions are indistinguishable from the complemented mutants (Figure 5C). As shown in Figure 6A, plastids of complemented mutants have a wild-type morphology, whereas mutant plants have undifferentiated plastids (Figure 6B). We concluded from these experiments that the *PAC* gene is entirely contained in the 8-kb XhoI genomic fragment. We used restriction fragment length polymorphisms and recombinant inbred lines (Reiter

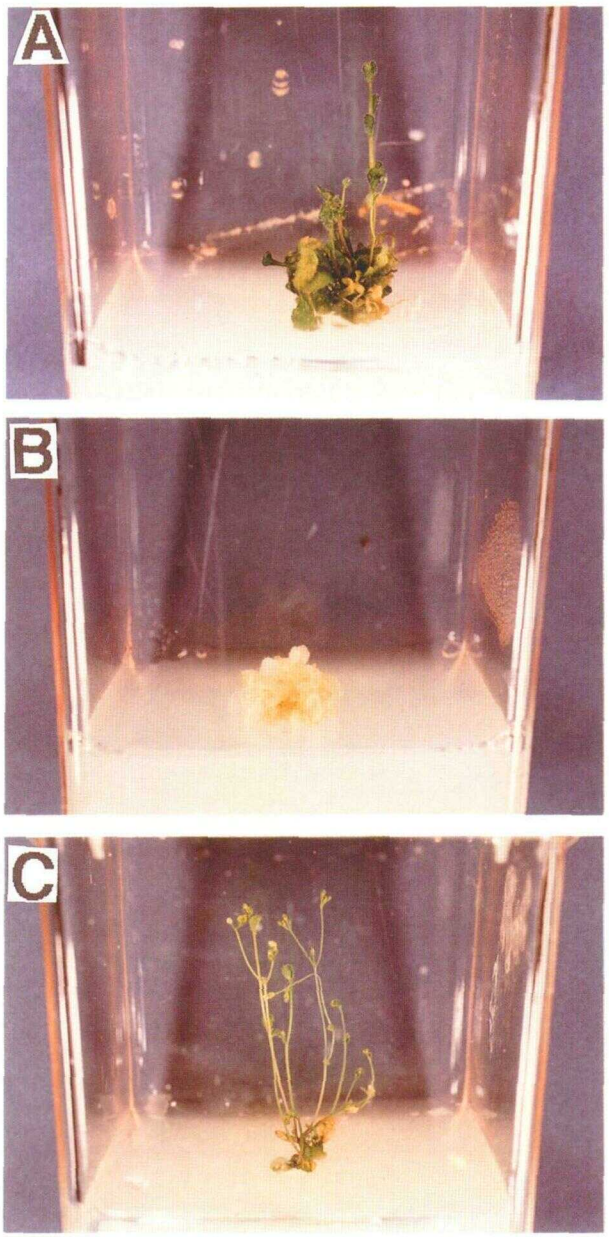

Figure 5. Complementation of the *pac* Mutation with Cloned Arabidopsis Genomic DNA Carrying the Wild-Type *PAC* Gene.

Plants were transformed and regenerated from root cultures as described in Methods.
(A) Homozygous *pac* plant transformed with the *PAC* gene.
(B) Homozygous *pac* plant transformed with the T-DNA plasmid vector.
(C) Wild-type control.

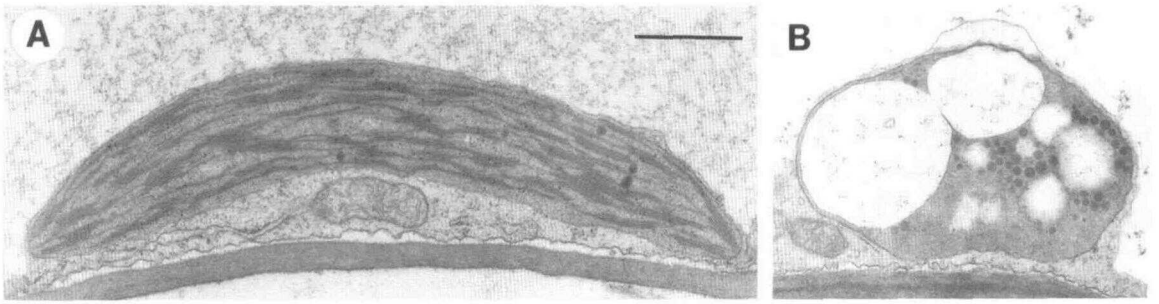

Figure 6. Plastid Ultrastructure in Complemented *pac* Plants.

(A) Chloroplast of a homozygous *pac* plant carrying the *PAC* transgene.
(B) *pac* control transformed with the plasmid vector.
Plastids were analyzed by TEM as described in Methods.
Bar in **(A)** = 1.0 μm and applies to both panels.

et al., 1992) to map this genomic fragment to the same region of chromosome 2.

Isolation and Characterization of *PAC* cDNAs

To characterize the *PAC* transcript, we screened cDNA libraries with a 1-kb wild-type genomic fragment amplified from the region corresponding to the site of T-DNA insertion. We identified three different classes of cDNAs (*PAC1*, *PAC2*, and *PAC3*) ranging in length from 1.1 to 3.0 kb. We sequenced 6.5 kb of genomic DNA and cDNAs from all three classes. Figures 7A and 7B show diagrams of the *PAC* gene and the three cDNAs. Comparison of the DNA sequences indicated that the various cDNAs correspond to differentially spliced transcripts. The *PAC* gene contains nine exons and eight introns. Exons 1, 2, 3, 5, and 6 are present in all three cDNAs, whereas exons 4 and 7 can be processed at alternative 5′ splice sites. By using

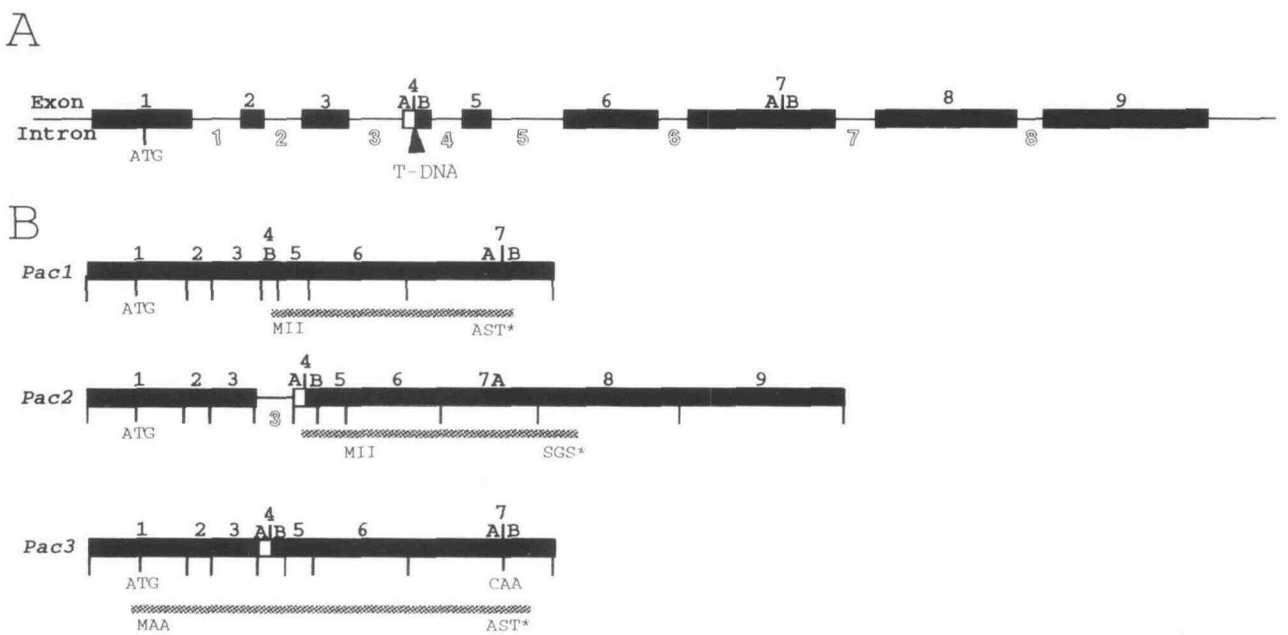

Figure 7. Genomic and cDNA Cloning of *PAC*.

(A) Structure of the genomic *PAC* region (2.75 kb), indicating exons, introns, and the location of the T-DNA insertion.
(B) Diagram of *PAC1* (1.0 kb), *PAC2* (1.9 kb), and *PAC3* (1.2 kb) cDNA clones showing the three N- and C-terminal amino acids of the predicted proteins in the one-letter code. A short predicted peptide starting at the exon 1 ATG of *PAC1* and *PAC2* is not shown.
Note the differential splicing of exon 4. Solid and open numbers indicate exons and introns, respectively. For exon 4, differentially spliced (4A) and constant (4B) regions are indicated.

reverse transcriptase–polymerase chain reaction (RT-PCR) to amplify polyadenylated *PAC* transcripts, we determined that there are several additional transcripts from this region (data not shown). At least in light-grown plants, *PAC3* is the predominant species (data not shown). However, we cannot exclude the possibility that other mRNAs may become more abundant at different stages of development or in response to environmental stimuli.

The open reading frames of the *PAC* transcripts cloned have the capacity to encode different predicted proteins. *PAC1* could encode a 168–amino acid protein. A product sharing the same N terminus but extending a further 29 residues at the C terminus can be predicted from *PAC2*. *PAC3* could encode a 310-residue protein extending to the in-frame exon 1 ATG (Figure 8). No open reading frame encoding more than 12 amino acids was detected 5′ of this initiation codon. PAC3 is an acidic (predicted charge and isolelectric point of −17 and 4.7, respectively) and highly charged protein (39% charged amino acid residues). As shown in Figure 9, two different secondary structure prediction algorithms suggest that the predominant structure of PAC is the α-helix.

A data base search using the BLAST service of the National Center for Biotechnology Information (Rockville, MD; Altschul et al., 1990) revealed that PAC3 is a novel protein with a low level of conservation (score 84, $P = 8.9^{-13}$) to the C-terminal half of human moesin (membrane-organizing extension spike protein) and the related proteins ezrin, radixin, and merlin (moesin-ezrin-radixin–like protein), the recently described candidate for the neurofibromatosis 2 tumor suppressor product (Trofatter et al., 1993; termed schwannomin in Rouleau et al., 1993). Searching the newly developed protein domain (ProDom) data base, created by organizing all entries in the SWISSPROT data base into homologous domains using the DOMAINER algorithm (Sonnhammer and Kahn, 1994), we detected conservation of PAC3 to the ProDom 761 sequence (score 83, $P = 3.6^{-13}$), a consensus of 11 mammalian proteins of the moesin-radixin-ezrin family. This domain of the moesin family of proteins interacts with actin (Algrain et al., 1993) and contains a high proportion of charged amino acids (38 to 43%) and an extensive α-helical conformation. Currently, we do not know whether this sequence conservation reflects similarities in function and/or evolutionary origin.

Control of Gene Expression in *pac*

We used RNA gel blot analysis to study the control of expression of the *PAC* gene in wild-type plants and of representative nuclear and plastid genes in the *pac* mutant. Figures 10A and 10B show that *PAC* expression is positively regulated by light (>10-fold induction) and is not affected by treatment with the carotenoid inhibitor norflurazon. Because of the low abundance of *PAC* transcripts in seedlings, this result had to be confirmed using quantitative RT-PCR (Figure 10B). No *PAC* transcripts were detected in mutant plants. The *pac* mutation does not affect the expression of the *CAB* nuclear gene family (Figure 10C), which encodes light-harvesting proteins, but decreases the expression of *PSBA*, a representative chloroplast gene (Figure 10D). As expected from previous reports, norflurazon treatment affects *CAB* and to a lesser extent *PSBA* gene expression (Taylor, 1989; Sagar and Briggs, 1990). Therefore, *PAC* is a light-regulated gene whose expression does not depend on chloroplast differentiation. Loss of *PAC* function, however, does not affect *CAB* expression.

```
TGAGCTACTAGTACTAAGCTACACCACGGGGTTTAATTTGTGAAATCCGAAACTAGGGAG   60

ACTAAATCCGAATAGATATAGATAGCCTAAGGGATTCGGGGCTGCAACAAAATCACTCCC  120

ACTCACTGCGAACGTCGACTATGGCGGCGACGTCGCTGGTTCTGACGTGCGCATCCCCTC  180
                  M  A  A  T  S  L  V  L  T  C  A  S  P  L     14

TATTCAGCAGCCCTCGGGTTATTTCTGCTACGAAGAAGCTGACTACAGAGTTGTCGATTT  240
F  S  S  P  R  V  I  S  A  T  K  K  L  T  T  E  L  S  I  S     34
   1
CTA|CAGCTAAATTCCGAAGAAGATGCTCGGGAAACAATGATGAAGTGCTTCTAGAAGGAA 300
T  A  K  F  R  R  R  C  S  G  N  N  D  E  V  L  L  E  G  M     54
                        2
TGCCACCGGAGTATTACGATGAT|GAATGGCAAGCTCGACAGAGAGAGAAGACCAAAGAAC 360
P  P  E  Y  Y  D  D  E  W  Q  A  R  Q  R  E  K  T  K  E  L     74

TGCGGCGGATGCAGCGGGAGGAAGAAGAAGAAGAGGAGAGAAAGATTGAAGAATACCGTG 420
R  R  M  Q  R  E  E  E  E  E  E  E  R  K  I  E  E  Y  R  E     94

AAATTGGCACGAGGTTGAAGGAATTTCCCGAGCAAGACTTAAGGAAAGCCAGAAAGCTCG 480
I  G  T  R  L  K  E  F  P  E  Q  D  L  R  K  A  R  K  L  V    114
                                 3
TCTCCAGCTTCATCAGAGCTGCCGAGGAAGTCGAA|GAGAGAATTGAAGAAGCAGCCGAGA 540
S  S  F  I  R  A  A  E  E  V  E  E  R  I  E  E  A  A  E  K    134
                              T-DNA
AAGGAGAACTTGACGAGCTTGTCCTCATGAT|CATATGGAACCGGCTTGACCTTGCTAGGC 600
G  E  L  D  E  L  V  L  M  I  I  W  N  R  L  D  L  A  R  R    154
      4                                                   5
GCGAT|GATGAGAAGGACGCCATCAGAAGTCTTGATCTTTTGTATAGAAGAGTCG|AGACAG 660
D  D  E  K  D  A  I  R  S  L  D  L  L  Y  R  R  V  E  T  E    174

AGATCTTAAAACGGCAAGCAAGTCCTGCAATGAAACTGCTGAATGATCTTCTAAATATGC  720
I  L  K  R  Q  A  S  P  A  M  K  L  L  N  D  L  L  N  M  H    194

ATGATGGCTTTGAAGACGATGCTTGGCTCAAGGACTGCAGAAAACGAATGGCTGAGACCT  780
D  G  F  E  D  D  A  W  L  K  D  C  R  K  R  M  A  E  T  F    214
                                                      6
TCCCCCGAGAAGACCCCTTCAGCATTCTAATGCCACCGGGATTCGACATTGATAT|GCATC 840
P  R  E  D  P  F  S  I  L  M  P  P  G  F  D  I  D  M  H  Q    234

AAGGACAGTTGCGACCGCCCATTGAGACTGAGACAGACAACACCCTTCTGAGAGTAGACT  900
G  Q  L  R  P  P  I  E  T  E  T  D  N  T  L  L  R  V  D  F    254

TTGTAAGAGAAGTGGATGCACTGCTACAGGAAGTGAGGATAGAGGAAGACGCTACAACTG  960
V  R  E  V  D  A  L  L  Q  E  V  R  I  E  E  D  A  T  T  G    274

GTAGCAAAGGAGAAGGGCTTGATCCTGAAGCTATAGCACTTAAGTTTAAGCAACAGGAGA 1020
S  K  G  E  G  L  D  P  E  A  I  A  L  K  F  K  Q  Q  E  K    294

AGCAACGAACCATCCGCCAAATTGAAGCCATTCTTGATTTAGCCTCAACTTGAAGTGGTA 1080
Q  R  T  I  R  Q  I  E  A  I  L  D  L  A  S  T  *             310

GGCAGTTAACTAGAATATCAATCTATACGCCATAATAATTTTTTTAAGATAGACCCTAGA 1140

GTTAGATTGATTCAGGCGTTTTTGTTTAGAAATGAATGGAGTCTAAATAATAGGTTTTGG 1200
```

Figure 8. Nucleotide and Deduced Peptide Sequence of *PAC3*.

The location of introns and the T-DNA insertion site are shown. The alternative start codon of *PAC1* and *PAC2* is indicated by a double underline. Numbers above the sequence indicate the location of introns. Underlined nucleotide bases correspond to the differentially spliced 4A region. The nucleotide sequence of *PAC3* has been submitted to GenBank as accession number L35241.

DISCUSSION

We have described an Arabidopsis mutant affected in the control of leaf and chloroplast development. We cloned and

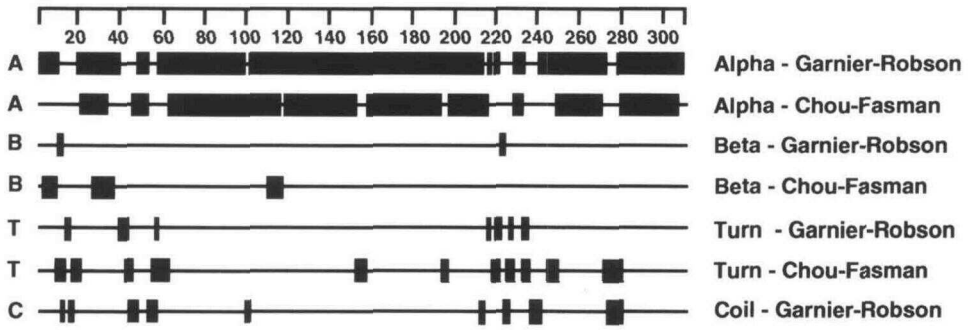

Figure 9. Secondary Structure Prediction of PAC.

Regions corresponding to α-helixes, β-sheets, turns, and coils were determined by the Chou-Fasman or Garnier-Robson algorithms using LaserGene (DNAstar; Madison, WI).

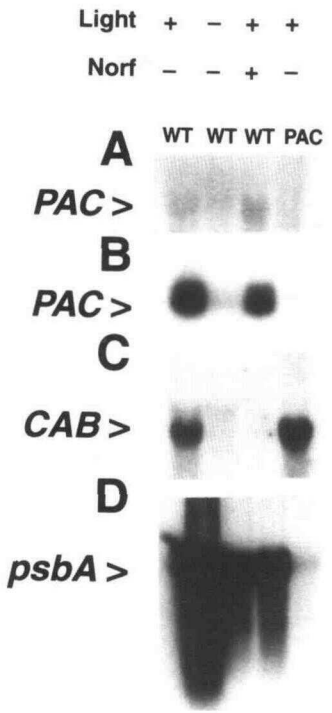

Figure 10. Control of Gene Expression in the *pac* Mutant.

Shown are autoradiograms of blots containing 10 μg of total RNA or RT-PCR products hybridized to the ^{32}P-labeled probes shown on the left.

(A) Total RNA, exposure time 16 hr.

(B) RT-PCR products, exposure time 40 min.

(C) Total RNA, exposure time 16 hr.

(D) Total RNA, exposure time 15 min.

RNA was extracted from 1-week-old wild-type (WT) or *pac* plants grown in light (+) or dark (−) in the presence (+) or absence (−) of 10^{-5} M Norflurazon (Norf) as indicated. For **(A)** and **(C)**, blots were exposed to x-ray film at −70°C with an intensifying screen. For **(B)** and **(D)**, exposures were done at room temperature.

mapped the corresponding gene and determined that it encodes a novel protein product. Early stages of *pac* leaf and chloroplast development are not significantly affected, but in later stages the *PAC* deficiency results in developmentally arrested plastids and altered leaf formation. Plastids in homozygous *pac* mutants undergo initial stages of differentiation from proplastids and etioplasts, but they do not develop into chloroplasts. Chlorophyll and carotenoids accumulate at low levels in the *pac* mutant in spite of the complete loss of gene function.

Using the T-DNA tag, we cloned *PAC* genomic DNA and confirmed that this DNA fragment contains the *PAC* gene by complementing the *pac* mutant. We determined that the *PAC* gene is differentially spliced and contains at least two functional polyadenylation signals. The most abundant transcript, *PAC3*, has the capacity to encode a hydrophilic protein of 36 kD that has a predicted α-helical structure. The structure of the gene suggests that *PAC* does not encode a pigment biosynthesis enzyme, but the corresponding protein may play a yet unknown role in the biosynthesis of chlorophylls and carotenoids. The low-level accumulation of photosynthetic pigments may result from either an effect of PAC on the biosynthesis of chlorophylls and carotenoids or a defect in the accumulation of pigments as a result of the impaired development of chloroplast membranes.

In early stages of development, both *pac* and wild-type leaves acquire the characteristic layered cell pattern. Therefore, up to stage 1 leaf development proceeds in the absence of chloroplast differentiation. In later stages, however, cells of the mutant palisade lose their typical shape, and the epidermal cells enlarge abnormally. Thus, the *pac* phenotype indicates the existence of a control of leaf maturation acting after the basic differentiation of leaf tissues. Leaf development is a precisely controlled developmental process influenced by environmental factors, primarily light. The formation of a layered photosynthetic organ from an undifferentiated primordium involves cell division, cell expansion, cell and organelle differentiation, and tissue formation (Steeves and Sussex, 1989).

To optimize photosynthesis, the structure of mature leaves must balance light intensity and evaporative load. Both light quality and quantity affect the size, shape, and morphology of leaves. The development of the palisade mesophyll exhibits considerable plasticity in response to light, temperature, water stress, and salt stress (Nobel and Walker, 1985; Dale, 1988; Moore, 1992). Thus, leaf development can be divided into an early, genetically programmed pattern formation stage and a later pattern expression stage that involves the final cell divisions and the acquisition of mature cell shapes and that depends primarily on environmental signals. If *PAC* is required for the final stages of leaf development, loss of this gene function may result in palisade cells losing their columnar shape to adopt a "default" spherical form. The chloroplast and leaf phenotypes may be mediated by a single *PAC* product or, as suggested by the alternative splicing detected at the locus, *PAC* may encode multiple proteins with different cellular localizations and functions. Currently, we do not know whether the leaf and chloroplast phenotypes are directly or indirectly controlled by *PAC*. If the chloroplast participates in the perception or processing of the environmental signals that modulate the differentiation of the leaf palisade, the leaf phenotype may be an indirect result of the chloroplast defect resulting from the loss of *PAC* function. Alternatively, the function of *PAC* may be to control cell differentiation through a process that is also required for organelle differentiation.

We have not found a description of similar mutants in the scientific literature, except for a variegated *Epilobium* mutant in which palisade cells in the white sectors have the morphology of spongy mesophyll and often show enlarged intercellular spaces (discussed in Tilney-Bassett, 1978). However, variegated green/white mutants may not be ideal to study this process because green sectors generally expand further than white areas, possibly generating physical forces that may result in aberrant morphologies.

PAC expression is regulated by light and is not affected by blocking chloroplast development with the bleaching herbicide norflurazon. The light regulation of *PAC* together with the function of the gene deduced from the phenotype of the *pac* mutant suggest that this gene participates in the modulation of leaf shape and chloroplast development by light. Unlike treatment with the bleaching herbicide norflurazon (Taylor, 1989), the genetic obstruction of chloroplast development induced by *PAC* does not block *CAB* gene expression.

METHODS

Plant Material

The *pale cress* (*pac*) mutant was isolated from a collection of T-DNA–mutagenized *Arabidopsis thaliana* ecotype Wassilewskija seed (Feldmann, 1991). Plants were grown in flats under standard greenhouse conditions using a 16-hr light/8-hr dark cycle or in 1% agar nutrient plates at 25°C under continuous cool-white and Gro-Lux illumination with an intensity of 75 to 95 $\mu E\ m^{-2}\ sec^{-1}$. Sterilization and plating of Arabidopsis seeds on agar plates was as previously described (Feldmann and Marks, 1987). Pigments were extracted from stage 1 plants and analyzed according to Lichtenthaler and Wellburn (1983).

Light Microscopy

To assay the effect of the *pac* mutation on internal leaf anatomy, transverse sections were taken from leaves fixed and embedded in Quetol resin (Howard and O'Donnell, 1987) for transmission electron microscopy (TEM; see below). Thick sections (2 to 3 μm) were attached to glass microscope slides using poly-L-lysine and stained for 8 min at 60°C in 0.1% toluidine blue O in 100 mM sodium acetate buffer, pH 4.5 (Jones and Rost, 1989). The length of each leaf and position of sections relative to the leaf base were recorded (Pyke et al., 1991). A total of 14 leaves of each wild type and mutant were sampled.

Quantitative data concerning the number of cells comprising the epidermis and mesophyll and the area occupied by these regions relative to the total cross-sectional area were obtained from micrographs printed to a final magnification of ×850. Data were collected only from sections positioned ~50 to 75% of total leaf length from the base and in regions lacking vascular tissue (i.e., interveinal areas). To compare leaf development, 10 micrographs derived from two to four samples of each stage were analyzed for each of two size classes (stage 1, 1.5 to 2.5 mm in length; stage 2, 4.0 to 5.0 mm in length) for both *pac* and wild-type leaves (a total of 40 micrographs).

Electron Microscopy

Tissue processed for TEM was derived from two experiments. To examine plastid differentiation, we processed mutant and wild-type leaves and shoot apices from 2-week-old plants. To examine de-etiolation, seeds were first germinated for 36 hr in an illuminated growth chamber, followed by growth in the dark for 5 days. The plants were then exposed to white light for 0, 0.5, 2, 4, 8, 12, and 24 hr before excising and processing the cotyledons.

Samples were fixed in 4% glutaraldehyde in 100 mM sodium cacodylate buffer, pH 7.2. Because of variation in the time required for manipulation of each sample prior to fixation, the duration of fixation varied between experiments. Fixation times at 4°C and subsequently at 23°C, respectively, were as follows for each experiment: plastid development, 2 to 5 and 4.5 hr; first de-etiolation experiment (12 and 24 hr), 3.5 and 3.0 hr; second de-etiolation experiment (0, 0.5, 2, 4, and 8 hr), 16.0 and 3.0 hr. Following aldehyde fixation, samples were postfixed in 2% osmium tetroxide in the same cacodylate buffer, stained in 1% aqueous uranyl acetate for 8 hr at 4°C, dehydrated in acetone, and embedded in either Spurr's or Quetol resin. A total of 73 leaves were sectioned for TEM; 10 to 40 leaves were used per experiment.

Genomic DNA Isolation

Frozen plant tissue was ground and incubated at 55°C for 1 hr with 100 μg/mL proteinase K, 100 mM Tris, pH 8, 100 mM EDTA, 250 mM NaCl, and 1% sarkosyl. Samples were centrifuged 10 min at 5000*g*, and the supernatant was placed in a new tube. DNA was precipitated by the addition of 0.6 volumes of isopropanol and 0.1 volume of 3 M NaOAc, pH 5.3. The DNA was pelleted by centrifugation for 15 min

at 8000*g*, redissolved in Tris-EDTA, and purified by CsCl banding (Lichtenstein and Draper, 1985).

Genomic Library Construction

Genomic DNA isolated from wild-type Arabidopsis (ecotype Wassilewskija) was partially digested with Sau3A and ligated to BamHI-digested and partially filled λGEM-11 arms (Promega). The ligated DNA was packaged using Gigapack II gold packaging extract (Stratagene). The packaged DNA was plated and amplified in *Escherichia coli* host KW251 (Promega) according to the manufacturer's instructions.

PAC Gene Cloning

Sterilized seeds from self-pollinated *pac* heterozygotes were germinated on agar plates (Murashige and Skoog, 1962). Homozygous *pac* seedlings were identified and transferred to flasks containing 50 mL of Murashige and Skoog salts with 1% sucrose and grown for 4 weeks with gentle shaking. Genomic DNA isolated from homozygous *pac* plants was used to clone a 12.7-kb fragment containing 6.3 kb of *pac* plant DNA via plasmid rescue. Genomic DNA fragments containing an intact *PAC* gene were cloned by using the rescued plant DNA to screen an Arabidopsis wild-type (ecotype Wassilewskija) genomic library in λGEM-11 by plaque hybridization.

DNA and RNA Gel Blot Hybridization

Genomic DNA for gel blot analysis was isolated from freeze-dried tissue by the method of Murray and Thompson (1980). The DNA was further purified by CsCl banding (Lichtenstein and Draper, 1985). RNA gel blots contained 20 μg of total RNA isolated according to Bartholomew et al. (1991). Quantitative reverse transcriptase–polymerase chain reaction (RT-PCR) was done according to Bartley and Scolnik (1993) using 35 cycles and primers 5′-TGAGCTACTAGTACTAAG-3′ and 5′-CGAGCCGTCGAGACTACTTCG-3′ and Arabidopsis phytoene desaturase (*PDS*) as an internal control.

PAC cDNA Cloning

A 6.5-kb fragment of genomic DNA containing the *PAC* gene and a portion of the plant DNA flanking the right border were sequenced via dideoxy termination using Sequenase enzyme (U.S. Biochemical Corp.) according to the manufacturer's instructions. A 1.1-kb PCR product surrounding the region of T-DNA insertion was amplified and used as a hybridization probe to screen an Arabidopsis cDNA library (Kieber et al., 1993). Two classes of cDNA were identified and sequenced as described above. Additional classes of cDNA were amplified by RT-PCR (Bartley and Scolnik, 1993). The most abundant product was cloned by blunt-end ligation into SmaI-digested pBluescript SK+ and sequenced as described above.

Transformation and Complementation of *pac*

The plasmid pRR101, containing a hygromycin resistance selectable marker regulated by the cauliflower mosaic virus 35S enhancer/promoter with a chlorophyll *a/b* binding protein (*cab*) leader sequence and a nopaline synthase (*nos*) 3′ termination sequence, was constructed by introducing the hygromycin expression cassette into the multiple-host binary plasmid pZS222. Plasmid pZS222 contains 24 bp of right and left border repeat sequences and an octopine synthase (*ocs*) enhancer sequence 5′ of the right border. An 8-kb XhoI fragment containing the entire *PAC* gene was subcloned into pRR101 to generate pRR108. Plasmid pRR108 was introduced into *Agrobacterium tumefaciens* GV3101::pMP90RK (Koncz et al., 1990) via electroporation. Root tissue from homozygous *pac* plants grown in flasks was used for cocultivation and transformation by Agrobacterium as described by Márton and Browse (1991) for Arabidopsis ecotype Columbia.

ACKNOWLEDGMENTS

We thank Michael Picollelli for the statistical analysis of leaf sections. We also thank Richard Howard for the advice on the interpretation of electron micrographs, Sandra Russell and Timothy Caspar for critical reading of the manuscript, Kenneth Feldmann for counsel in the early stages of this work, Joseph Ecker (University of Pennsylvania, Philadelphia) for the gift of a cDNA library, and Mary Locke (Du Pont) for the hygromycin expression cassette and the binary plasmid pZS222.

Received April 15, 1994; accepted July 18, 1994.

REFERENCES

Algrain, M., Turunen, O., Vaheri, A., Louvard, D., and Arpin, M. (1993). Ezrin contains cytoskeleton and membrane binding domains accounting for its proposed role as a membrane-cytoskeletal linker. J. Cell Biol. **120,** 129–139.

Altschul, S.F., Gish, W., Miller, W., Myers, E.W., and Lipman, D.J. (1990). Basic local alignment search tool. J. Mol. Biol. **217,** 403–410.

Bartholomew, D.M., Bartley, G.E., and Scolnik, P.A. (1991). Abscisic acid control of *rbcS* and *cab* transcription in tomato leaves. Plant Physiol. **96,** 291–296.

Bartley, G.E., and Scolnik, P.A. (1993). cDNA cloning, expression during development, and genome mapping of *PSY2*, a second tomato gene encoding phytoene synthase. J. Biol. Chem. **268,** 25718–25721.

Dale, J.E. (1988). The control of leaf expansion. Annu. Rev. Plant Physiol. Plant Mol. Biol. **39,** 267–295.

Feldmann, K.A. (1991). T-DNA insertion mutagenesis in *Arabidopsis*: Mutational spectrum. Plant J. **1,** 71–82.

Feldmann, K.A., and Marks, M.D. (1987). *Agrobacterium*-mediated transformation of germinating seeds of *Arabidopsis thaliana*: A non-tissue culture approach. Mol. Gen. Genet. **208,** 1–9.

Hou, Y., von Arnim, A.G., and Deng, X.-W. (1993). A new class of Arabidopsis constitutive photomorphogenic genes involved in regulating cotyledon development. Plant Cell **5,** 329–339.

Howard, R.J., and O'Donnell, K.L. (1987). Freeze substitution of fungi for cytological analysis. Exp. Mycol. **11,** 250–269.

Jones, T.J., and Rost, T.R. (1989). Histochemistry and ultrastructure of rice (*Oryza sativa*) zygotic embryogenesis. Am. J. Bot. **76,** 504–520.

Kieber, J.J., Rothenberg, M., Roman, G., Feldmann, K.A., and Ecker, J.R. (1993). *CTR1*, a negative regulator of the ethylene response pathway in *Arabidopsis*, encodes a member of the Raf family of protein kinases. Cell **72,** 427–441.

Kirk, J.T.O. (1978). The nature of plastids. In The Plastids, J.T.O. Kirk and R.A.E. Tilney-Bassett, eds (New York: Elsevier), pp. 3–6.

Koncz, C., Mayerhofer, R., Koncz-Kalman, Z., Nawrath, C., Reiss, B., Rédei, G.P., and Schell, J. (1990). Isolation of a gene encoding a novel chloroplast protein by T-DNA tagging in *Arabidopsis thaliana.* EMBO J. **9,** 1337–1346.

Lichtenstein, C., and Draper, J. (1985). Genetic engineering of plants. In DNA Cloning, Vol. II, D.M. Glover, ed (Washington, D.C.: Academic Press), pp. 67–119.

Lichtenthaler, H.K., and Wellburn, A.R. (1983). Determination of total carotenoids and chlorophylls *a* and *b* of leaf extracts in different solvents. Biochem. Soc. Trans. **11,** 591–592.

Márton, L., and Browse, J. (1991). Facile transformation of Arabidopsis. Plant Cell Rep. **10,** 235–239.

Mayfield, S.P., and Taylor, W.C. (1987). Chloroplast photooxidation inhibits the expression of a set of nuclear genes. Mol. Gen. Genet. **208,** 309–314.

Moore, P.D. (1992). A leaf for all seasons. Nature **360,** 110–111.

Murashige, T., and Skoog, F. (1962). A revised medium for rapid growth and bioassays with tobacco tissue cultures. Physiol. Plant. **15,** 473–497.

Murray, M.G., and Thompson, W.F. (1980). Rapid isolation of high molecular weight plant DNA. Nucl. Acids Res. **8,** 4321–4325.

Nobel, P.S., and Walker, D.B. (1985). Structure of leaf photosynthetic tissue. In Photosynthetic Mechanisms and the Environment, J. Barber and N.R. Baker, eds (Amsterdam: Elsevier), pp. 501–536.

Pyke, K.A., Marrison, J.L., and Leech, R.M. (1991). Temporal and spatial development of the cells of the expanding first leaf of *Arabidopsis thaliana* (L.) Heynh. J. Exp. Bot. **42,** 1407–1416.

Reiss, T., Bergfeld, R., Link, G., Thien, W., and Mohr, H. (1983). Photooxidative destruction of chloroplasts and its consequences for cytosolic enzyme levels and plant development. Planta **159,** 518–528.

Reiter, R.S., Williams, J.G.K., Feldmann, K.A., Rafalski, J.A., Tingey, S.V., and Scolnik, P.A. (1992). Global and local mapping in *Arabidopsis thaliana* by using recombinant inbred lines and random amplified polymorphic DNAs. Proc. Natl. Acad. Sci. USA **89,** 1477–1481.

Rouleau, G.A., Merel, P., Lutchman, M., Sanson, M., Zucman, J., Marineau, C., Hoang-Xuan, K., Demczuk, S., Desmaze, C., Plougastel, B., Pulst, S.M., Lenoir, G., Bijlsma, E., Fashold, R., Dumanski, J., de Jong, P., Parry, D., Eldridge, R., Aurias, A., Delattre, O., and Thomas, G. (1993). Alteration in a new gene encoding a putative membrane-organizing protein causes neurofibromatosis type 2. Nature **363,** 515–521.

Sagar, A.D., and Briggs, W.R. (1990). Effects of high light stress on carotenoid-deficient chloroplasts in *Pisum sativum*. Plant Physiol. **94,** 1663–1670.

Sonnhammer, E.L.I., and Kahn, D. (1994). Modular arrangement of proteins as inferred from analysis of homology. Protein Sci. **3,** 482–492.

Staehelin, L.A. (1986). Chloroplast structure and supramolecular organization of photosynthetic membranes. In Encyclopedia of Plant Physiology, A. Pirson and M.H. Zimmermann, eds (Berlin: Springer-Verlag), pp. 1–84.

Steeves, T.A., and Sussex, I.M. (1989). Organogenesis of the shoot. In Patterns in Plant Development, T.A. Steeves and I.M. Sussex, eds (New York: Cambridge University Press), pp. 150–172.

Taylor, W.C. (1989). Regulatory interactions between nuclear and plastid genomes. Annu. Rev. Plant Physiol. Plant Mol. Biol. **40,** 211–233.

Tilney-Bassett, R.A.E. (1978). Recognition of sorting-out. In The Plastids, J.T.O. Kirk and R.A.E. Tilney-Bassett, eds (New York: Elsevier), pp. 358–359.

Trofatter, J.A., MacCollin, M.M., Rutter, J.L., Murrell, J.R., Duyao, M.P., Parry, D.M., Eldridge, R., Kley, N., Menon, A.G., Pulaski, K., Haase, V.H., Ambrose, C.M., Munroe, D., Bove, C., Haines, J.L., Martuza, R.L., MacDonald, M.E., Seizinger, B.R., Short, M.P., Buckler, A.J., and Gusella, J.F. (1993). A novel moesin-, ezrin-, radixin-like gene is a candidate for the neurofibromatosis 2 tumor suppressor. Cell **72,** 791–800.

Zhang, H., Scheirer, D.C., Fowle, W.H., and Goodman, H.M. (1992). Expression of antisense or sense RNA of an ankyrin repeat–containing gene blocks chloroplast differentiation in Arabidopsis. Plant Cell **4,** 1575–1588.